JOURNAL OF SUSTAINABLE MATERIALS PROCESSING AND MANAGEMENT
e-ISSN: 2821-2843

JSMPM

Vol. 4 No. 1 (2024) 89-105
https://publisher.uthm.edu.my/ojs/index.php/jsmpm

Application of Taguchi Methods and Regression Analysis to Optimize Process Parameters and Reinforcements for Maximizing Composite's Coefficient of Friction for Brake Disc Application: A Statistical Optimization Approach

Tanimu Kogi Ibrahim[1]*, Ibrahim Iliyasu[2], Popoola Caleb Abiodun[3]

[1] *Mechanical Engineering Department, Faculty of Engineering*
Federal University Wukari, Katsina-Ala Road, Wukari, Taraba State, PMB 1020, NIGERIA

[2] *Mechanical Engineering Department*
Ahmadu Bello University, Sokoto Road, Samaru-Zaria, Zaria 2222 Kaduna, NIGERIA

[3] *Chemical Engineering Department, Faculty of Engineering*
University Wukari, Katsina-Ala Road, Wukari, Taraba State, PMB 1020, NIGERIA

*Corresponding Author: terrytanimu@yahoo.com
DOI: https://doi.org/10.30880/jsmpm.2024.04.01.008

Article Info

Received: 22 May 2024
Accepted: 20 June 2024
Available online: 26 June 2024

Keywords

Coefficient of friction, aluminum matrix composite, nonsynthetic reinforcements, optimization, brake disc

Abstract

This research aimed to explore the potential of pumice and coal ash as natural reinforcements for aluminum alloy (AA6061) composites, with a focus on optimizing the coefficient of friction of the composite for brake disc production. The pumice, coal ash, and aluminum alloy were characterized using X-ray fluorescence (XRF), X-ray diffraction (XRD), thermogravimetric analysis (TGA), and scanning electron microscopy (SEM). The Taguchi method was employed to design the experimental runs and to identify optimal process parameters and reinforcements for maximizing the composite's coefficient of friction. At the same time, regression analysis was utilized to establish a robust mathematical model for predicting the composite's coefficient of friction based on the process variables. The XRF characterization results revealed that aluminum alloy (AA6061) contained Al, Si, and Mg as the major elements. The analysis also shows that the predominant constituents in coal ash were Si, Al, Fe, Ti, and Ca, whereas that of brown pumice particulates were Si, Fe, Al, Ca, K, and Ti. The XRD characterization analysis revealed that brown pumice and coal ash consist of SiO_2, Fe_2O_3, and Al_2O_3 as the major phases, making them well-suited as reinforcement in metal matrixes. According to the thermogravimetric and differential thermal analyses, the aluminum alloy, brown pumice, and coal ash have an onset temperature of 264.08, 724 °C, and 606.61°C, respectively, before deterioration. The optimal composite's coefficient of friction of 0.661 (experimental) was achieved at 2.5vol% of brown pumice, 10 vol% of coal ash, 400 rpm stirrer speed, 700 °C pouring temperature, and 15 minutes stirring duration. The developed mathematical model shows an excellent level of coefficient of friction prediction, with an R-squared value of 99.42%, 97.82%, and 76.40% for R-square, adjusted R-square, and predicted R-square, respectively.

1. Introduction

The safety and control of a vehicle hinges on the efficacy of its braking system. Disc brakes, with their superior heat dissipation compared to drum brakes, have become the dominant technology in modern automobiles. During braking, a complex interplay of forces occurs at the interface between the brake pads and the disc. Friction, a fundamental force arising from the interaction of two surfaces, plays a critical role in this process. The coefficient of friction (CoF) between the pads and disc directly governs the braking force generated and ultimately determines the vehicle's stopping distance and overall braking performance [1-4].

Conventional brake discs are primarily manufactured from cast iron. While cast iron offers good wear resistance and thermal stability, its CoF can be susceptible to variations in temperature and operating conditions. This phenomenon can lead to inconsistencies in braking performance and contribute to brake fade [3].

Aluminum alloy (AA6061), on the other hand, possesses several advantages for brake disc applications. It is significantly lighter in weight compared to cast iron, leading to improved vehicle handling and fuel efficiency. Additionally, the alloy exhibits superior thermal conductivity, promoting efficient heat dissipation and potentially mitigating brake fading. However, pure aluminum alloy lacks the necessary mechanical strength and wear resistance required for high-performance braking applications [5,6].

To address these limitations, researchers are exploring the development of aluminum matrix composites (AMCs) for brake discs. The utilization of aluminum composites in brake disc manufacturing has garnered significant attention due to their lightweight nature and impressive mechanical properties. By integrating aluminum composites into brake disc design, manufacturers can achieve a desirable balance between strength, thermal conductivity, and weight reduction, ultimately leading to improved vehicle performance and addressing challenges related to brake disc wear and thermal management [7]. AMCs combine the favorable thermal properties of aluminum with the enhanced mechanical characteristics offered by reinforcement materials. By incorporating suitable reinforcements, we can potentially develop brake discs with a higher CoF that remains stable across a wider operating temperature range [8].

The quest for sustainable and cost-effective materials has led researchers to explore nonsynthetic reinforcements such as pumice, coal, and red mud as alternatives to synthetic materials in aluminum composites. These materials are often by-products or waste from other industrial processes, providing an environmental and economic advantage [7].

Pumice, a volcanic rock, offers low density and high porosity, which can enhance the thermal insulation properties of the composite while maintaining adequate mechanical strength. Coal, particularly in its fly ash form, provides a fine particulate reinforcement that can improve wear resistance and thermal stability [9,10]. Similarly, coal ash, a by-product of coal carbonization, contains mineral components that reinforce brake disc materials and improve thermal stability [10,11]. By harnessing these natural renewable materials, automotive manufacturers can create brake discs that are not only high-performing and cost-effective but also environmentally friendly and sustainable. This shift towards non-synthetic reinforcements underscores the industry's commitment to greener manufacturing practices. It aligns with broader sustainability initiatives aimed at reducing environmental footprint while maintaining product performance and safety standards [12]. Using these nonsynthetic materials not only reduces the reliance on expensive synthetic reinforcements but also promotes recycling and waste management, aligning with sustainable development goals. However, the variability in the properties of these natural materials requires meticulous processing and characterization to ensure consistency and performance in the final composite [10,13].

Double stir casting is a widely used method for producing aluminum matrix composites due to its simplicity, cost-effectiveness, and ability to produce near-net shape components. This process involves the incorporation of reinforcements into the molten aluminum matrix through mechanical stirring, which helps in achieving a uniform distribution of particles and enhancing the composite's properties [14-16]. The double stir casting technique typically involves two stages of stirring: the first stage occurs at a lower temperature to improve the wetting of the reinforcement particles by breaking the gas layers surrounding it. The second stage is performed at a higher temperature to promote better particle dispersion and minimize porosity. Parameters such as Stirrer speed, duration, temperature, and reinforcement addition rate are critical to achieving a homogeneous composite with optimal properties. The efficiency of this process lies in its ability to produce composites with fine and uniformly distributed reinforcements, which are essential for achieving desired mechanical and thermal properties in brake disc applications. Proper control of the process parameters can significantly influence the final properties of the composite, including the coefficient of friction, wear resistance, and thermal conductivity [17].

Optimizing the production parameters of aluminum composites is crucial for enhancing their performance in brake disc applications. The Taguchi method and regression analysis are powerful statistical tools used for this purpose. Taguchi's method involves designing experiments to systematically vary process parameters and identify the optimal settings that result in the desired properties. This approach minimizes the number of

experiments required while providing robust data on the influence of each parameter [18,19]. In the context of brake disc composites, the Taguchi method can be used to optimize variables such as the type and amount of reinforcement, Stirrer speed, temperature, and duration [16,20]. The goal is to achieve a composite with a high specific heat capacity, which is essential for effective heat dissipation during braking. A higher specific heat capacity allows the brake disc to absorb more thermal energy without a significant rise in temperature, thus enhancing performance and longevity [21].

Regression analysis complements the Taguchi method by providing a mathematical model that describes the relationship between the process parameters and the composite properties [22]. This model can be used to predict the outcomes of different parameter settings and identify the most influential factors. By combining these two approaches, researchers can fine-tune the production process to achieve composites with optimal thermal and mechanical properties for brake disc applications.

This research intends to develop a robust framework for improving the AMC's coefficient of friction via the synergistic integration of Taguchi methodology and regression analysis, seeking to advance sustainable materials for automotive applications, thereby paving the way for greener and more efficient transportation systems. The main goals include the characterization and production of pumice, coal ash, and Al-CA-PB composites, optimizing process parameters and natural reinforcements (pumice and coal ash) using Taguchi methods to enhance produced AMC's coefficient of friction, establishing predictive models through regression analysis to elucidate the relationships between variables and coefficient of friction, and using ANOVA to determine the impact of factors and interactions on AMC's coefficient of friction.

2. Materials and Methods

2.1 Materials

The materials used to produce the Al-BP-CA hybrid composite are coal, brown pumice (BP), and aluminum alloy (AA6061). The coal was acquired from a coal mine in Effeche-Akpalli, Benue State, Nigeria. The brown pumice was also extracted from an underground mining site in Biu, Borno State, Nigeria.

2.2 Brown Pumice Particulates Production Process

The brown pumice was washed and dried for 48 hours at 100 °C to remove filth and moisture. Respectively. The aggregated were pulverized with a laboratory mortar and pestle before being processed into powders using a ball milling machine. This production technique is consistent with the research results of Ibrahim *et al.* [23] and Jayakrishnan and Ramesan [24]. The brown pumice particulates were further sieved per BSI 377:1990 standard into three different particle sizes (90 µm, 56 µm, and 25 µm).

2.3 Production of Coal Ash Particulates

The coals were washed and dried for 48 hours at 100 °C to remove moisture and filth before pulverizing them using a jaw crusher. The pulverized coals were put in a crucible made of graphite and subjected to heating to about 1100 °C in an electrical furnace without any air for 8 hours. After being normalized in the oven, it was processed into powders using a ball milling machine. This method is supported by research by Hassan and Gomes [9] and Sharma *et al.* [25]. The generated carbonized coal underwent further sieving per BSI 377:1990 standard to produce carbonized coal ash particles 25, 53, and 90 µm particle size.

2.4 Experimental Design

Taguchi's design methodology was used to plan experimental runs. In this study, five factors: brown pumice particulate (A) (wt%), coal ash particles (B) (wt%), stirrer speed (C) (rpm), pouring temperature (D) (°C), and stirring duration (D) (min) with four different levels were considered to be studied as shown in Table 1.

Table 1 *Reinforcements and stir casting process parameters factors and levels*

S/N	Processing Factors	Unit	Factors Designation	Level			
				1	2	3	4
1	Brown Pumice	wt%	A	2.5	5	7.5	10
2	coal Ash	wt%	B	2.5	5	7.5	10
3	Stirrer Speed	rpm	C	200	300	400	500
4	Pouring Temperature	°C	D	700	750	800	850
5	Stirring Duration	min	E	5	10	15	20

The reinforcement, stirrer speed, pouring temperature, and stirring duration limits and levels were selected, referencing previous studies conducted by Adebisi and Ndaliman [26] and Ibrahim et al. [10]. Minitab 19 software was employed to create the L16 orthogonal array for the 16 experimental trials, shown in Table 2.

Table 2 *L_{16} orthogonal array for production of hybrid composite*

Experimental Run	Factors				
	A (vol%)	B (vol%)	C (rpm)	D (°C)	E (min)
1	2.5	2.5	200	700	5
2	2.5	5	300	750	10
3	2.5	7.5	400	800	15
4	2.5	10	500	850	20
5	5	2.5	300	800	20
6	5	5	200	850	15
7	5	7.5	500	700	10
8	5	10	400	750	5
9	7.5	2.5	400	850	10
10	7.5	5	500	800	5
11	7.5	7.5	200	750	20
12	7.5	10	300	700	15
13	10	2.5	500	750	15
14	10	5	400	700	20
15	10	7.5	300	850	5
16	10	10	200	800	10

2.5 Al-BP-CA Hybrid Composites Fabrication

The composites were produced using a two-step stir casting procedure described by Ikubanni *et al.* [27] and Adediran *et al.* [28] using a bottom pouring stir casting machine at SwamEquip, Chennai, India.

Prior to the casting process, the brown pumice and coal ash particles underwent a preheating treatment for 2 hrs at 500 °C per the recommendations of previous investigations by Kumar *et al.* [29] and Adebisi *et al.* [30] to oxidize and calcine the particle surfaces. Subsequently, the aluminum alloys (AA6061) were fed into the furnace and heated to 800 °C to guarantee thorough alloy melting. Before incorporating the preheated reinforcements, the surface dross was initially eliminated. Afterward, 0.01% NaCl (to eliminate gases) and 1% magnesium powders (to enhance wettability) were introduced into the molten aluminum [14]. The liquid alloy undergoes controlled cooling within the furnace until it reaches a temperature of 610 °C, transitioning into a semisolid state. Subsequently, an automated stainless-steel stirrer coated with a protective layer was lowered into the melted aluminum alloy in the furnace to initiate stirring to form a vortex within the melt. The preheated particulate materials were introduced gradually into the molten slurry at a steady flow rate of 5 grams per minute. Subsequently, the mixture was reheated to the prescribed pouring temperature, stirrer speed, and time as specified in the experimental run of the design plan. The mold was heated to around 450 °C before pouring the slurry into it [31].

For each of the experimental trials, this methodology was adhered to, with careful consideration of the process parameters and the reinforcement percentage as recommended in the design plan [26]. A control (without reinforcement) was also produced to compare the effects of the reinforcement.

2.6 Characterization of the Constituents

Both matrix (aluminum AA6061) and reinforcement (brown pumice and coal ash) were characterized using XRF, SEM-EDS, XRD, and TGA/DTA to determine their chemical composition, morphology, crystalline structure, and thermal stability.

2.7 Specific Wear Rate

This test complies with ASTM G 99-17 (ASTM, 2017) standard utilizing a pin-on-disc tribometer computer integrated wear & friction monitor TR-201CL (Ducom make). Wear and CoF tests were conducted by exerting a force of 8 Newton at a constant speed of 10 cm/s and 50 m sliding distance. The CoFs were then recorded by the machine [8,23].

2.8 Statistical Analysis and Optimization

The Al-BP-CA composites' specific wear rates were analyzed experimentally using Taguchi optimization and ANOVA with the aid of Minitab software version 21.4.2. The study employed a "larger-the-better" objective function in Taguchi optimization to optimize the process parameters that can give us the best composite's specific wear rate [19].

The confidence interval for this analysis was evaluated using Equation 1.

$$C.I. = \sqrt{f_{\propto(1,d_e)} v_e \left(\frac{1}{m} + \frac{1}{n}\right)} \quad (1)$$

Where 1 is the F Distribution Critical Values (α=0.05 significance level) between 1 and d_e(which is the degree of freedom of error), gotten from statistical tables, v_e is the variance (mean square) of error, which are obtained from the analysis of variance. N is the number of effective replications. M was evaluated using Equation 2.

$$M = \frac{Total\ number\ of\ experiment}{1 + degree\ of\ freedom\ of\ control\ factors} \quad (2)$$

3. Results and Discussion

3.1 Constituting Materials' XRF

The Constituents (aluminum alloy (AA6061), brown pumice, and coal ash particles) of the Al-BP-CA hybrid composites were examined via an XRF analyzer. Tables 3 and 4 present the results of the investigation. The XRF results of the aluminum alloy, as displayed in Table 3, indicate that aluminum, silicon, and magnesium are the predominant constituents. This finding corroborates the findings of Kareem *et al.* [5] and Ibrahim *et al.* [18].

Table 3 *Aluminum's XRF results*

Element	Al	Si	Fe	Cu	Mn	Mg	Zn	Cr	Ti	Ca	others
vol%	97.74	0.61	0.44	0.16	0.02	0.82	0.01	0.07	0.01	0.05	0.07

Table 4 shows the XRF results of the coal ash and pumice particulates. The analysis verified that coal particle ash predominantly consisted of Si, Al, Fe, Ti, and Ca. The major constituents of brown pumice particulates were Si, Fe, Al, Ca, K, and Ti. These outcomes are similar to investigations by Ibrahim *et al.* [10] and Dagwa and Adama [32]. The presence of these elements indicates that brown pumice and coal ash particulates have the potential to serve as effective particulate reinforcements in metal matrices given their chemical composition, which shares similarities with certain agricultural and industrial residue (bagasse, Coconut fiber ash, and Banana fibers ash, fly ash, bottom ash, and red mud) [9,32].

Table 4 *BP and CA chemical composition*

S/n	Elements	Brown pumice (%)	Coal ash particles (%)
1	O	42.267	46.52
2	Al	7.907	7.556
3	Si	20.594	22.141
4	P	0.288	0.000
5	S	0.074	4.415
6	Cl	0.718	1.721
7	K	4.212	1.130
8	Ca	8.574	2.667
9	Ti	2.140	3.500
10	V	0.084	0.140
11	Cr	0.008	0.170
12	Mn	0.198	0.268
13	Fe	12.348	8.910

14	Co	0.070	0.062
15	Ni	0.010	0.066
16	Cu	0.046	0.147
17	Zn	0.029	0.014
18	Zr	0.157	0.322
19	Nb	0.050	0.054
20	Mo	0.002	0.011
21	Ag	0.027	0.031
22	Ba	0.186	0.123
23	Ta	0.012	0.035

3.2 Constituting Materials' XRD

Based on the XRD patterns of brown particles (BP) displayed in Fig. 1, it is evident that the patterns include peaks corresponding to an amorphous quartz (SiO_2) material, along with specific crystalline phases of anorthite ($Ca\ Al_2(SiO_4)_2$) and albite ($NaAlSi_3O_8$). These findings correlate with Ersoy *et al.* [33] and Pinarci and Kocak [34] findings. Upon matching the coal ash particles, distinct phases of SiO_2, graphite(C), and muscovite ($KAl_2(AlSi_3O_{10})(F,OH)_2$) were identified, as shown in Fig. 1. This observation aligns with the research conducted by Ibrahim *et al.* [9] and Sahajwalla *et al.* [35], who identified some of these compounds in coal ash.

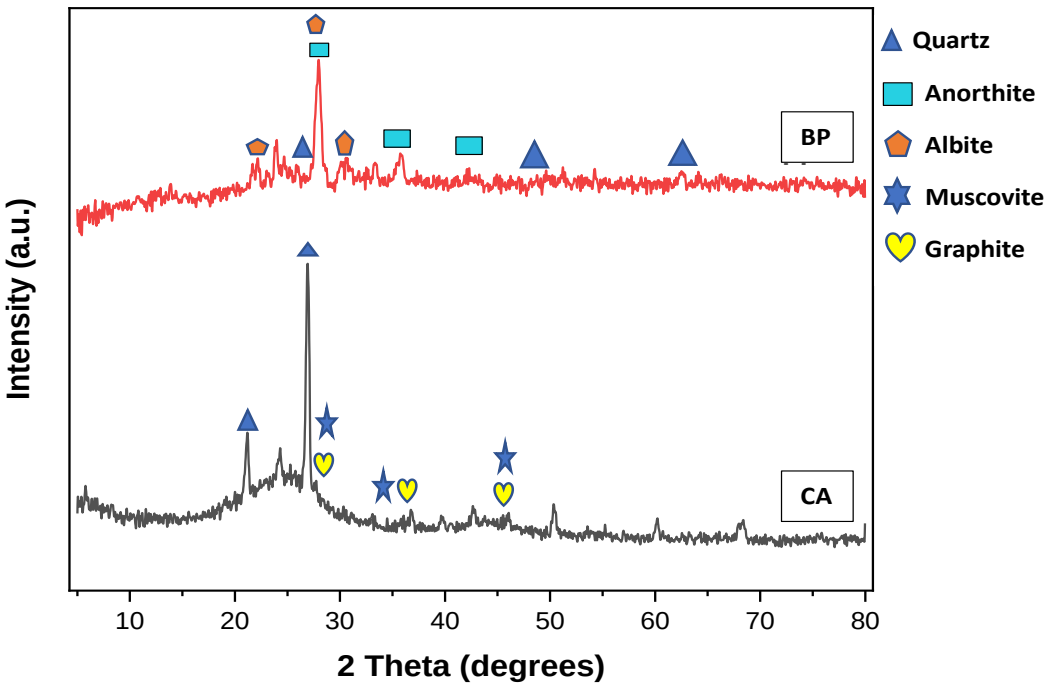

Fig. 1 *XRD results of BP and CA particles*

3.3 Thermogravimetric and Derivatives of Thermal Analysis of Aluminum Alloy

The TGA-DTA curves in Fig. 2 demonstrate a two-step weight loss for aluminum alloy when heated from 30 °C to 1000 °C in a nitrogen atmosphere. The TGA curve in the figure shows a significant drop until it is parallel to the temperature axis at approximately 513 °C.

The initial 1.16% weight loss occurs between a temperature of 83.29 and 264.08 °C, which can be linked to the evaporation of the absorbed surface moisture and some volatile matter. The major decompositions of the materials occur in one stage between the temperatures of 264.08 and 513 °C with a mass loss of 81.2%.

J. of Sustainable Materials Processing and Management Vol. 4 No. 1 (2024) p. 89-105

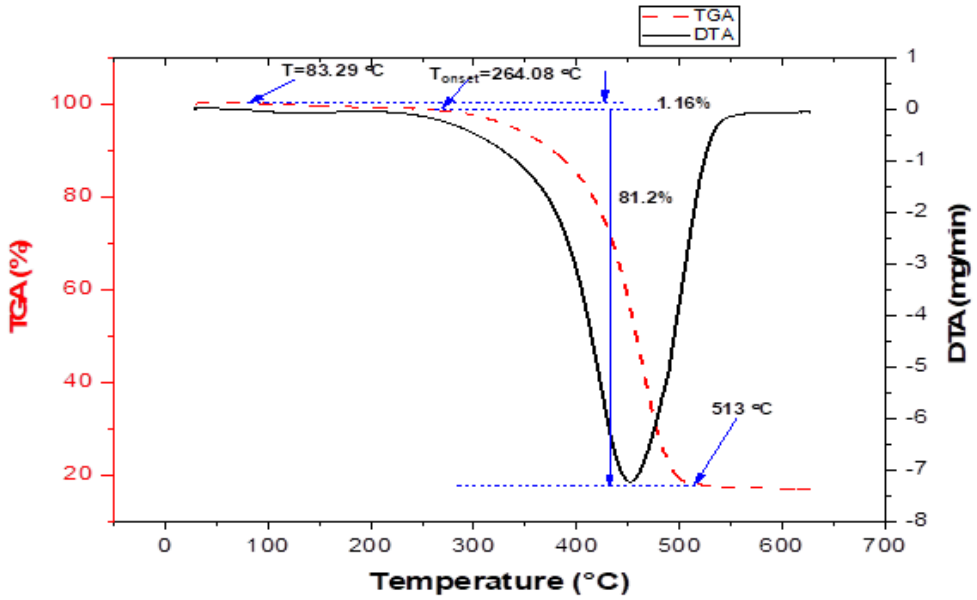

Fig. 2 *TGA-DTA curves of the aluminum alloy (AA6061)*

3.4 Thermogravimetric and Derivatives of Thermal Analysis of Brown Pumice Particulates

The TGA-DTA curves in Fig. 3 depict a two-step weight loss pattern for brown pumice particulates when exposed to a nitrogen gas atmosphere and heated within the temperature range of 30°C to 1000°C. The TGA curve in the Fig. 3 demonstrates a substantial decline until it aligns parallel to the temperature axis around 957 °C.

The initial 0.46% weight loss occurs between a temperature of 495.54 and 724 °C was observed, which can be linked to the evaporation of the absorbed surface moisture and some volatile matters. The major decompositions of the materials occur in one stage between 724 and 957 °C with a mass loss of 11.26%. The major decompositions in pumice can be accredited to the thermal decomposition of volatile substances such as sulfur dioxide (SO_2), carbon dioxide (CO_2), nitrogen, and various trace gases that may be present in the volcanic environment during the rock's formation. The lower mass loss in brown pumice particulates is owing to its high melting points (1343 °C) and the presence of TiO_2 (1843 °C) and SiO_2 (1710 °C), the major constituents, compared to the lower melting temperature of the aluminum alloy. This observation is similar to the work of Gencel [36].

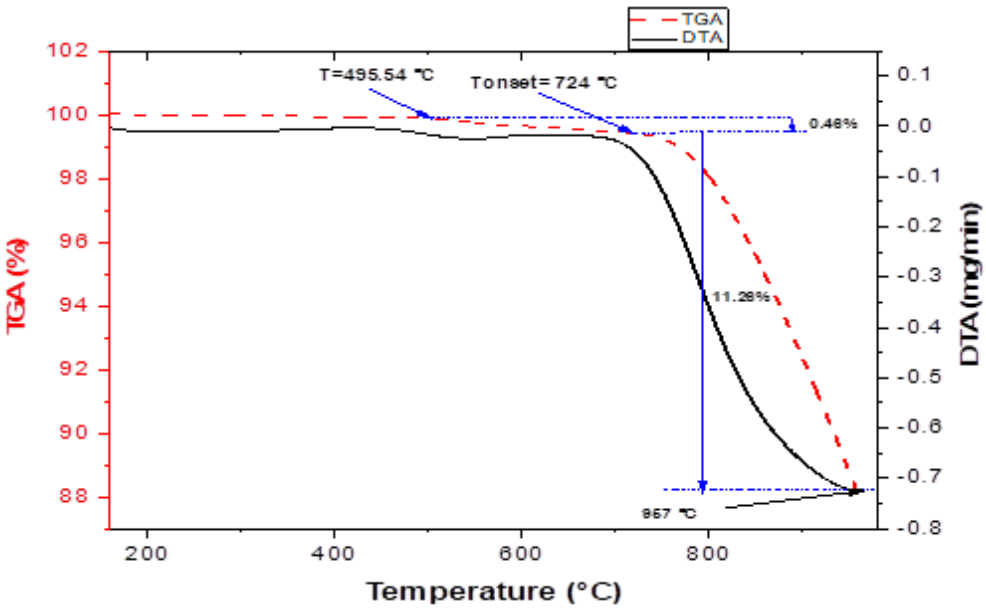

Fig. 3 *TGA-DTA curves of the brown pumice particle*

3.5 Thermogravimetric and Derivatives of Thermal Analysis of Coal Ash Particulates

The TGA-DTG curves in Fig. 4 demonstrate a three-step weight loss for coal ash particulates when exposed to a nitrogen gas atmosphere and heated within the temperature range of 30°C to 1000°C. The TGA curve in the figure shows a significant drop until it becomes parallel to the temperature axis at approximately 980.04 °C.

The initial 1.2% weight loss occurs between a temperature of 238.67 and 605.51 °C observed, which can be linked to the evaporation of the absorbed surface moisture and volatile matter. The major decompositions of coal ash particulates occur in two stages: in the temperature range of 605.51 °C to 840.52 °C, resulting in a mass reduction of 13.68%. Subsequently, the second phase occurred between 840 °C and 980.4 °C, with a mass loss of 24.38%. The first stage of major decomposition in coal ash particulates can be attributed to the volatile components such as water, hydrocarbons, or other gases trapped within the coal particles. The second stage might be due to the decomposition of carbonated minerals into oxides, which release carbon dioxide (CO_2) gas. The reduced mass loss in coal ash particulates is attributed to the elevated melting points of their primary constituents, TiO_2 and SiO_2 (1843°C and 1710°C, respectively), in comparison to the lower melting temperature of the aluminum alloy.

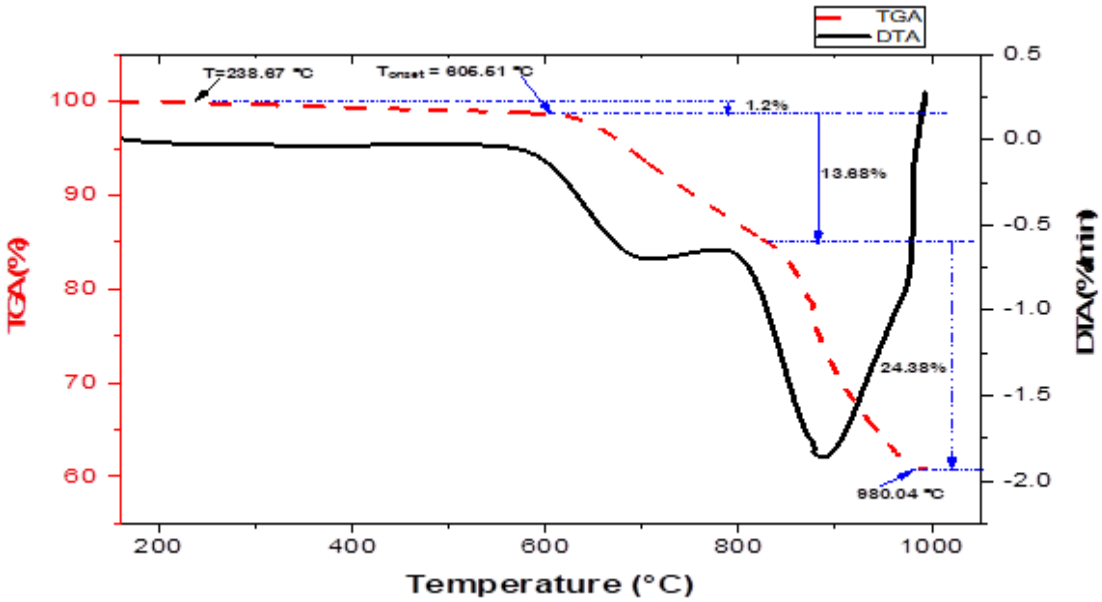

Fig. 4 *TGA-DTA curves of the coal ash particle*

3.6 Coefficient of Friction (CoF) of Al-PP-CC Hybrid Composite

Table 5 shows the results of a coefficient of friction test performed on sixteen hybrid composites and a control sample, along with their signal-to-noise ratios. From Table 5, the value of the coefficient of friction (CoF) of the as-cast aluminum alloy is greater than the value for all 16 runs. This phenomenon can be due to the inclusion of pumice and carbonated coal particles into the matrix, which consists of hard minerals and solid lubricants (graphite), as shown in the XRD results in Fig. 1. A similar trend has been observed by Veeravalli *et al*. [37] and Ujah *et al*. [38]; they show that the composites have a lower coefficient of friction than that matrix material when a stiffer reinforcement is used.

3.7 Taguchi Optimization of Reinforcements Casting Process Parameters

The higher-the-better objective function was used to observe the optimum and the most influential process parameters in the casting of aluminum hybrid composite. This analysis gave signal-to-noise ratios, main effect plots for the mean of the response, and the main effect plot for mean of signal-to-noise ratios, as presented in the discussions below.

3.8 Effect of Stir Casting Process Parameters on the Coefficient of Friction

The effect of pumice particles, carbonated coal particles, stirrer speed, pouring temperature, and stirring duration on the coefficient of friction are shown from Fig. 5 to Fig. 9, respectively.

J. of Sustainable Materials Processing and Management Vol. 4 No. 1 (2024) p. 89-105

Table 5 *Coefficient of friction test results and their respective signal to noise ratios*

Runs	Factors					Coefficient of friction	
(S/N)	Brown pumice (wt%)	Coal ash (wt%)	Stirrer speed (rpm)	Pouring temperature (°C)	Stirring duration (min)	Mean	S/N ratio (dB)
1	2.5	2.5	200	700	5	0.60	4.44
2	2.5	5	300	750	10	0.59	4.64
3	2.5	7.5	400	800	15	0.62	4.07
4	2.5	10	500	850	20	0.52	5.76
5	5	2.5	300	800	20	0.58	4.70
6	5	5	200	850	15	0.51	5.85
7	5	7.5	500	700	10	0.50	5.99
8	5	10	400	750	5	0.61	4.25
9	7.5	2.5	400	850	10	0.57	4.82
10	7.5	5	500	800	5	0.49	6.23
11	7.5	7.5	200	750	20	0.53	5.55
12	7.5	10	300	700	15	0.61	4.27
13	10	2.5	500	750	15	0.53	5.56
14	10	5	400	700	20	0.61	4.35
15	10	7.5	300	850	5	0.45	6.97
16	10	10	200	800	10	0.55	5.19
Mean						0.5542	5.17
	Control (As Cast)					0.63	

3.8.1 Effect of Pumice Particles on Coefficient of Friction

The effect of pumice particles on the coefficient of friction of the reinforced aluminum composite is shown in Fig. 5. The CoF of the hybrid composite decreases with increased pumice particles. This decrease in the coefficient of friction may be attributed to the good interfacial bonding of the ceramics with the aluminum matrix. Also, the hard crystalline characteristics of the pumice particles may be the source of surface property improvement, whereby the coefficient of friction is reduced. This study aligns with Veeravalli *et al*. [37] and Ujah *et al*. [38], who reported that the CoF AMCs decrease with increased wt% of reinforcement. The optimum coefficient of friction of 0.582 was observed at a 2.5 wt% pumice particle content.

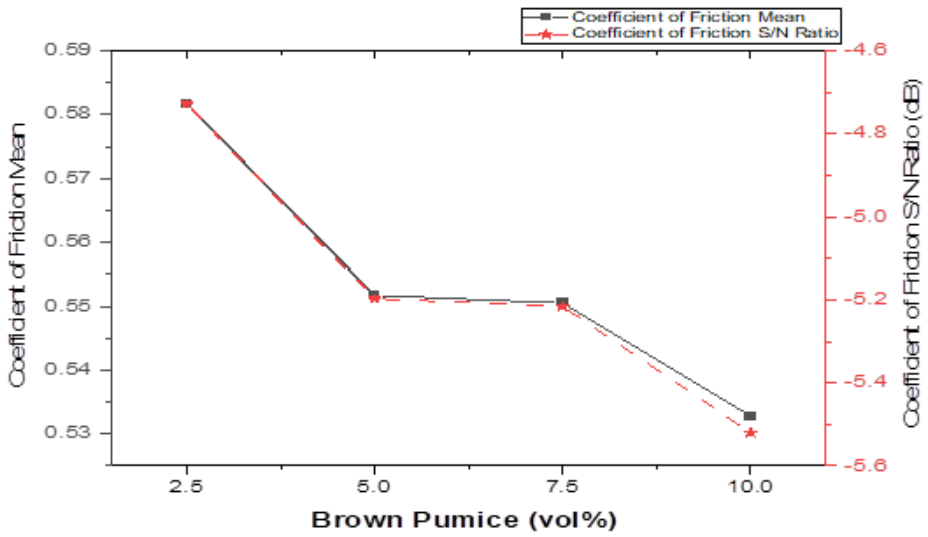

Fig. 5 *Variation of brown pumice content on the CoF of the aluminum hybrid composite*

3.8.2 Effect of Carbonated Coal Particles on Coefficient of Friction

Fig. 6 shows the decreasing effect of carbonated coal particle content on the coefficient of friction of the developed composites. It generally shows that between the content of 2.5% and 7.5%, there is no improvement in the aluminum metal matrix composite's surface properties (coefficient of friction). The highest coefficient of friction due to carbonated coal particles was 0.573, which was observed at 10 wt% content of the carbonated coal particle; the decrease can be attributed to the poor interfacial bonding between the matrix and the carbonated coal particles. Also, the decrease can be due to the presence of graphite in the carbonated coal particle, as shown in the XRD results, which acts as a solid lubricant. Beyond this content, the coefficient of friction was observed to increase with the increasing content of the carbonated coal particle. The subsequent increase trend can be due to the poor wettability of the carbonated coal particle, which can lead to insufficient interfacial bonding between it and the matrix. This study agrees with the finding made by Baradeswaran and Perumal [39] and Baradeswaran *et al*. [40]; they observed that CoF decreases to the minimum as reinforcement increases, then increases as the reinforcement increases beyond that point.

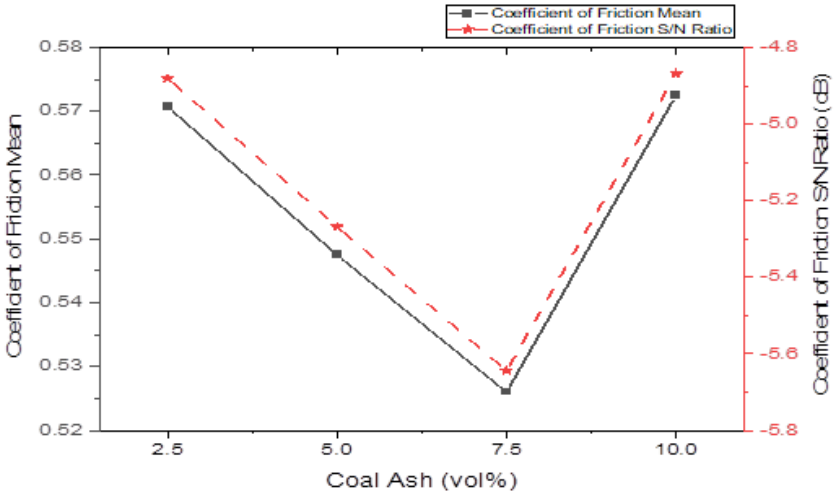

Fig. 6 *Variation of coal ash content on the CoF of the aluminum hybrid composite*

3.8.3 Effect of Stirrer Speed on Coefficient of Friction

Fig. 7 shows the effect of stirrer speed on the coefficient of friction of the developed aluminum hybrid composite material. It is observed that the coefficient of friction increased with the increase in stirrer speed from 200 to 400 rpm; this can be due to the homogenous distribution of the pumice and carbonated coal particles at a lower speed.

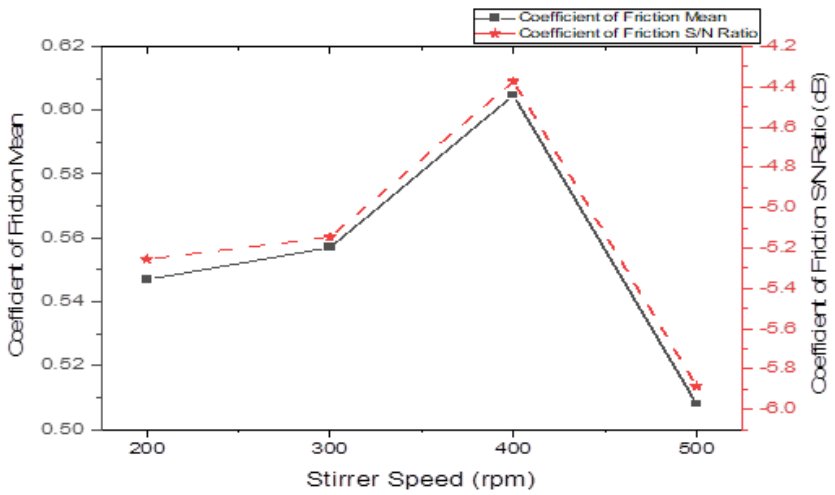

Fig. 7 *Variation of stirrer speed on the CoF of the aluminum hybrid composite*

Although beyond the stirrer speed of 400 rpm, the friction coefficient decreased as the stirrer speed increased. In contrast, the decrease might be attributed to the improper mixing of the reinforcement particles in the aluminum alloy matrix, which can be attributed to the increased agitation severity of the slurry, resulting in the clustering of the pumice and carbonated coal particles and entrapment of gas bubbles. These results agree with the findings of Prabu *et al*. [41]. An optimum coefficient of friction of 0.605 was observed at a stirrer speed of 400 rpm.

3.8.4 Effect of Stirring Temperature on Coefficient of Friction

Fig. 8 shows the effect of processing temperature on the coefficient of friction. The Figure shows that the coefficient of friction reduces with increased processing temperature. This reduction may be attributed to the ease of reinforcement settlement at a less viscous matrix due to higher temperatures. The optimum coefficient of friction of 0.580 was observed at a processing temperature of 700 °C.

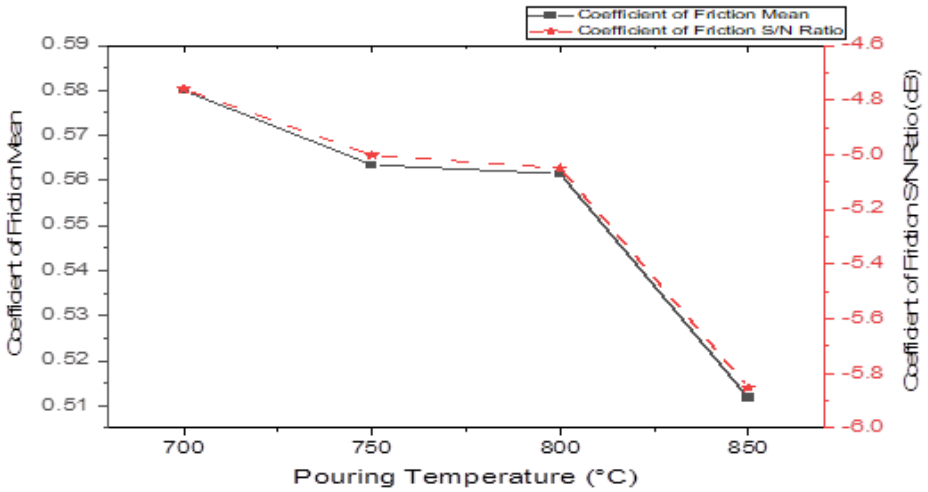

Fig. 8 *Variation of processing temperature on the CoF of the aluminum hybrid composite*

3.8.5 Effect of Stirring Duration on Coefficient of Friction

Fig. 9 shows the variation in the coefficient of friction strength with stirring duration for the hybrid aluminum composite. As shown in the figure, as the stirring duration increases, the coefficient of friction also increases and approaches the optimal value of 0.569 at a stirring duration of 15 min; beyond this point, the coefficient of friction decreases as the stirring duration increases.

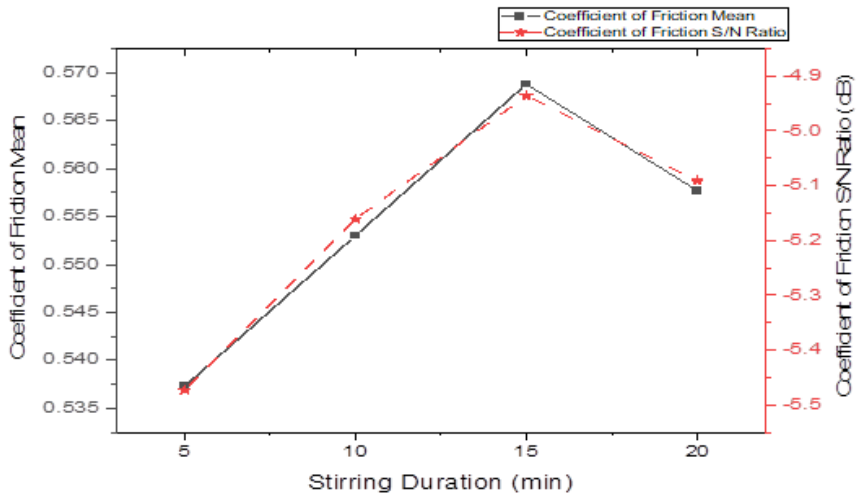

Fig. 9 *Variation of stirring duration on the CoF of the aluminum hybrid composite*

The increase can be attributed to the proper mixing of the reinforcements, leading to its homogeneous distribution in the matrix. However, the decrease can be attributed to a longer stirring duration, which increases the absorption of gases and oxidation in the liquid aluminum matrix, leading to the formation of porosity and blow holes. From the analysis, an optimum coefficient of friction of 0.569 was observed at a stirring duration of 15 mins.

3.9 Optimum Combination for Coefficient of Friction

The optimum reinforcements and process parameters of stir casting that give the best coefficient of friction are brown pumice particulates (A) content at 2.5 wt%, coal ash particulates (B) at 10 wt%, with a stirrer speed (C) of 400 rpm, at a pouring temperature (D) of 700 °C, and stirring duration (E) of 15 minutes which could be denoted as A_1-B_4-C_3-D_1-E_3.

3.10 Estimating the Optimal Coefficient of Friction

The predicted optimum coefficient of friction of 0.6546 for the aluminum hybrid composites based on the best combination of optimum control factors was obtained.

3.11 Confirmation Test

The result of the coefficient of friction confirmation test is shown in Table 6. From the Table, an average coefficient of friction of 0.661 was obtained. The CoF curve obtained from the wear test of the optimal and the control samples results is displayed in Fig. 10. Interestingly, the optimal sample has a higher CoF 0.661 compared to the latter (0.63).

Table 6 *Coefficient of friction test confirmation result*

Runs	Factors					Coefficient of friction			
(S/N)	Brown pumice (vol%)	Coal ash (vol%)	Stirrer speed (rpm)	Pouring temperature (°C)	Stirring duration (min)	Trial 1	Trial 2	Trial 3	Ave.
1	2.5	10	400	700	15	0.661	0.663	0.659	0.661

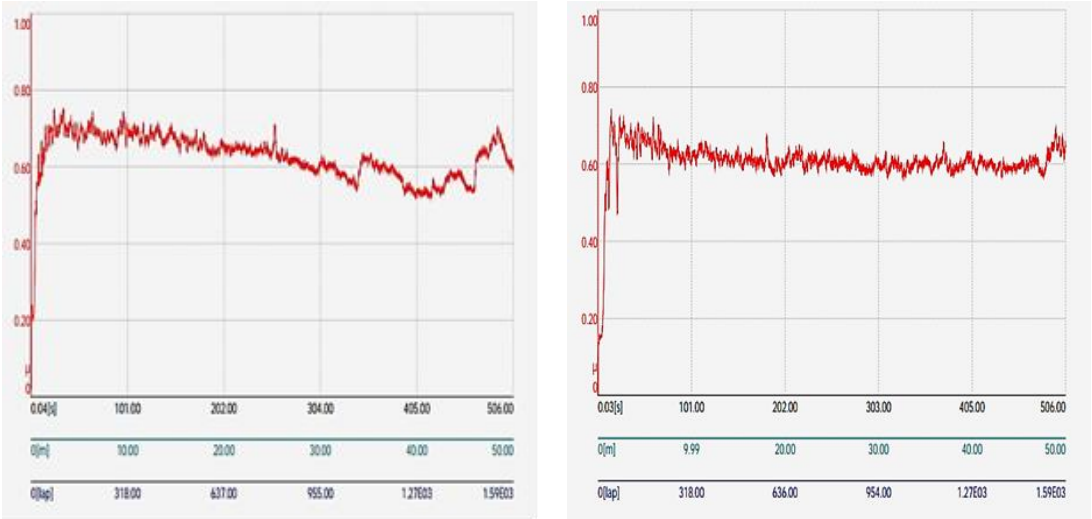

(a) **(b)**

Fig. 10 *CoF curve (a) Optimal; (b) Control sample*

The results of the predicted and experimental coefficient of friction values of the optimal processing parameters (A_1-B_4-C_3-D_1-E_3) of the hybrid aluminum matrix composite are shown in Table 7, where the percentage error was also calculated.

Table 7 *Confirmatory results comparison at the optimal level*

	Optimal process parameter settings	Predicting value	Experimental value	% Error
S/N ratio (dB)	A_1-B_4-C_3-D_1-E_3	-3.6805	-3.6	-2.35
CoF		0.6546	0.661	0.97

J. of Sustainable Materials Processing and Management Vol. 4 No. 1 (2024) p. 89-105

3.12 Regression Analysis (Modelling)

Table 8 shows that the regression model, all the factors, and the interactions significantly affected the coefficient of friction of the produced composite with a p-value less than 0.05.

Table 8 *Analysis of variance of the coefficient of friction for the hybrid composite*

Source	DF	Adj SS	Adj MS	F-Value	P-Value	% Contribution
Regression	11	0.041985	0.003817	62.19	0.001	
Brown Pumice (A)	1	0.00719	0.00719	117.15	0.000	10.91
Coal Ash (B)	1	0.003325	0.003325	54.18	0.002	5.04
Stirrer Speed (C)	1	0.013075	0.013075	213.03	0.000	19.84
Pouring Temperature (D)	1	0.005982	0.005982	97.46	0.001	9.08
Stirring Duration (E)	1	0.005918	0.005918	96.43	0.001	8.98
B*B	1	0.003147	0.003147	51.27	0.002	4.77
C*C	1	0.011396	0.011396	185.67	0.000	17.29
A*C	1	0.003161	0.003161	51.5	0.002	4.8
A*D	1	0.007526	0.007526	122.62	0.000	11.42
B*C	1	0.002167	0.002167	35.31	0.004	3.29
B*B*B	1	0.002782	0.002782	45.33	0.003	4.22
Error	4	0.000246	0.000061			0.37
Total	15	0.065915				100

The model for the coefficient of friction prediction derived from the regression analysis is shown by Equation 3.

$$\begin{aligned} CoF = {} & -2.067 + 0.5882A - 0.2734B + 0.002744C + 0.003723D - 0.01584E + 0.04586B^2 - 0.000003C^2 \\ & -0.000145AC - 0.000708AD - 0.000063BC - 0.002297B^3 \end{aligned} \quad (3)$$

The capability of the developed regression model was checked using a coefficient of determination R-square (R^2), R-square (adj), and R-square (pred). The model has a very high value of 99.42%, 97.82%, and 76.40% for R-square (R^2), R-square (adj), and R-square (pred), respectively. These values show a good fit between the coefficient of friction and the factors (stir process parameters and reinforcements) since they are close to 100%. Dan-Asabe [42] and Sivaiah & Chakradhar [43] show that an R-Square value greater than 75% is deemed adequate, implying a good fit between the response and the process parameters. The developed model adequately predicts the experimental and interpolated values, respectively. However, the difference of 21.42 % between the R-square (adjusted) and R-square (pred), which is just above the benchmark, inferred a fairly good prediction of 76.40 % outside the experimental region (extrapolation) [42,44]. Fig. 11. shows the comparison between the coefficient of friction data generated using the model equation (Equation 3) and the experimental values for the 16 different runs.

3.13 Confidence Interval (CI)

A confidence interval value of ± 0.0475 was evaluated using Equation 4. The obtained coefficient of friction result from the confirmatory test shows that the experimental value (0.6610) lies between the confidence interval range of the coefficient of friction, as shown below:

$$\begin{aligned} CoF_{predictive} - CI < CoF_{experimental} < CoF_{predictive} + CI \\ 0.6275 < CoF_{experimental} < 0.6945 \end{aligned} \quad (4)$$

This result confirms the acceptability of the optimum coefficient of friction prediction within the confidence interval of 95%.

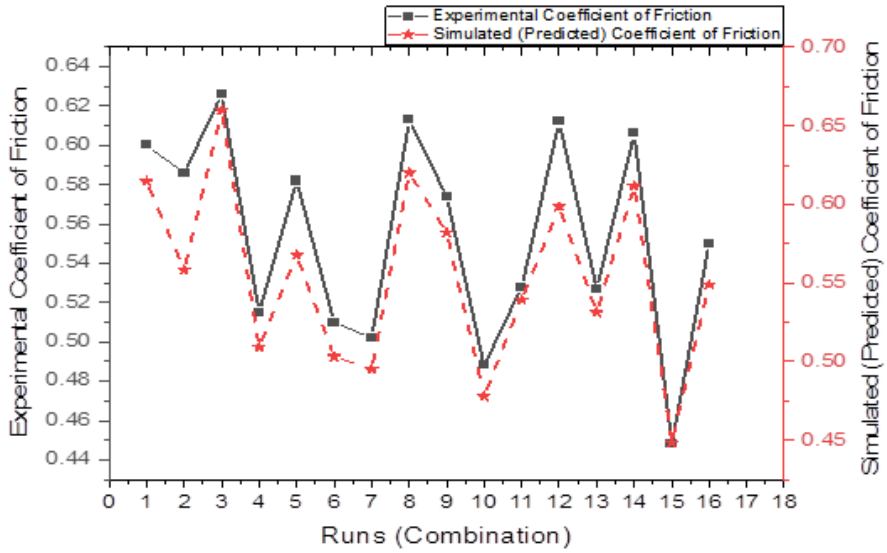

Fig. 11 *Experimental and predictive coefficient of friction*

4. Conclusion

This research aimed to explore the potential of pumice and coal ash as natural reinforcements for Al-CA-PB composites, with a focus on optimizing the coefficient of friction of the composite. The Pumice, coal ash, and composite were successfully developed and characterized. Taguchi methods and Regression analysis were employed to identify optimal process parameters for maximizing composite CoF and to establish a robust model to predict composite CoF based on the process variables. Based on these analyses, the following conclusions are drawn:

i. The XRF characterization results revealed that aluminum alloy (AA6061) contained aluminum, silicon, and magnesium. The predominant constituents in coal ash are Si, Al, Fe, Ti, and Ca, whereas that of brown pumice particulates were Si, Fe, Al, Ca, K, and Ti.
ii. The XRD analysis revealed that pumice and coal ash contained hard and stiff minerals such as SiO_2, Fe_2O_3, and Al_2O_3, making them suitable as reinforcements in metal matrixes.
iii. The thermogravimetric and differential thermal analyses demonstrated that the aluminum alloy, brown pumice, and coal can withstand high temperatures of up to 264.08, 724 °C, and 606.61°C, respectively, before any significant deterioration.
iv. The Taguchi optimization effectively identified optimal process parameters and reinforcements for maximizing the composite's CoF. An optimal coefficient of friction of 0.661 (experimental) was obtained using 2.5vol% of brown pumice, 10 vol% of coal ash, 400 rpm stirrer speed, 700 °C pouring temperature, and 15 minutes of stirring duration.
v. The developed mathematical model demonstrated an excellent level of prediction for the SHC of the composites based on the process parameters and ceramics reinforcement, with 99.27%, 97.25%, and 88.12%, as R-Square and adjusted R-Square, and predicted R-Square values, respectively.

Acknowledgement

The authors would like to express their sincere thanks and appreciation to the Federal University Wukari, Taraba State and Ahmadu Bello University Zaria, Kaduna State, Nigeria for the enabling environment provided for this research work.

Conflict of Interest

Authors declare that there is no conflict of interests regarding the publication of the paper.

Author Contribution

The authors confirm contribution to the paper as follows: ***study conception and design:*** *Tanimu Kogi Ibrahim, Ibrahim Iliyasu;* ***data collection:*** *Ibrahim Iliyasu;* ***analysis and interpretation of results:*** *Tanimu Kogi Ibrahim, Ibrahim Iliyasu;* ***draft manuscript preparation:*** *Tanimu Kogi Ibrahim, Ibrahim Iliyasu, Popoola Caleb Abiodun. All authors reviewed the results and approved the final version of the manuscript.*

References

[1] Aguilar Esteva, L. C., Kasliwal, A., Kinzler, M. S., Kim, H. C., & Keoleian, G. A. (2021). Circular economy framework for automobiles: Closing energy and material loops. Journal of Industrial Ecology, 25(4), 877-889.

[2] Ibrahim, M. A. (2013). A Study on Various Type of Rotor Disc Brake Using Fae Analysis. Doctoral dissertation, UMP.

[3] Fu, P. R. K. (2014). Study and development of novel composite materials for the application of car brake rotor. Doctoral dissertation, Curtin University.

[4] Wakeel, S., Bingol, S., Bashir, M. N., & Ahmad, S. (2021). Selection of sustainable material for the manufacturing of complex automotive products using a new hybrid Goal Programming Model for Best Worst Method–Proximity Indexed Value method. Proceedings of the Institution of Mechanical Engineers, Part L: Journal of Materials: Design and Applications, 235(2), 385-399.

[5] Kareem, A., Qudeiri, J. A., Abdudeen, A., Ahammed, T., & Ziout, A. (2021). A review on AA 6061 metal matrix composites produced by stir casting. Materials, 14(1), 175. https://doi.org/10.3390/ma14010175

[6] Sharma, A. K., Bhandari, R., Aherwar, A., Rimašauskienė, R., & Pinca-Bretotean, C. (2020). A study of advancement in application opportunities of aluminum metal matrix composites. Materials Today: Proceedings, 26, 2419-2424.

[7] Bodunrin, M. O., Alaneme, K. K., & Chown, L. H. (2015). Aluminium matrix hybrid composites: a review of reinforcement philosophies; mechanical, corrosion and tribological characteristics. Journal of materials research and technology, 4(4), 434-445. https://doi.org/10.1016/j.jmrt.2015.05.003

[8] Hemanth, J. (2009). Development and property evaluation of aluminum alloy reinforced with nano-ZrO2 metal matrix composites (NMMCs). Materials Science and Engineering: A, 507(1-2), 110-113.

[9] Hassan, M., & Gomes, V. G. (2018). Coal derived carbon nanomaterials–Recent advances in synthesis and applications. Applied Materials Today, 12, 342-358.

[10] Ibrahim, T. K., Yawas, D. S., Dan-Asabe, B., & Adebisi, A. A. (2023). Taguchi optimization and modelling of stir casting process parameters on the percentage elongation of aluminium, pumice and carbonated coal composite. Scientific Reports, 13(1), 2915. https://doi.org/10.1038/s41598-023-29839-8

[11] Zhou, H., Bhattarai, R., Li, Y., Si, B., Dong, X., Wang, T., & Yao, Z. (2022). Towards sustainable coal industry: Turning coal bottom ash into wealth. Science of the Total Environment, 804, 149985.

[12] Kumar, M. A., Seetharamu, S., Nayak, J., & Satapathy, L. N. (2014). A study on thermal behavior of aluminum cenosphere powder metallurgy composites sintered in microwave. Procedia Materials Science, 5, 1066-1074. https://doi.org/10.1016/j.mspro.2014.07.398

[13] Joshi, R., & Kuntanahal, R. (2020). Studies on Bottom ash strengthened LM13 composite. Materials Today: Proceedings, 20, 217-221. https://doi.org/10.1016/j.matpr.2019.11.119

[14] Aigbodion, V. S. (2012). Development of Al-Si-Fe/Rice husk ash particulate composites synthesis by double stir casting method. Usak University Journal of Material Sciences, 1(2).

[15] Adebisi, A. A., & Ndaliman, M. B. (2015, October). Mathematical modelling of stir casting process parameters for AlSiCp composite using central composite design. In Proceedings of the 28th AGM and International Conference of the Nigerian Institution for Mechanical Engineers organized by The Nigerian Institution for Mechanical Engineers. Nigeria, Abuja City.

[16] Adebisi, A. A., Maleque, M. A., & Ndaliman, M. B. (2016). Influence of Stirring Speed on Microstructure and Wear Morphology of SiCp-6061Al Composite. International Journal of Engineering Materials and Manufacture, 1(1), 21-26.

[17] Vinod, B., Ramanathan, S., Ananthi, V., & Selvakumar, N. (2019). Fabrication and characterization of organic and in-organic reinforced A356 aluminium matrix hybrid composite by improved double-stir casting. Silicon, 11, 817-829.

[18] Ibrahim, T. K., Yawas, D. S., Danasabe, B., & Adebisi, A. A. (2023). Optimization and statistical modeling of the thermal conductivity of a pumice powder and carbonated coal particle hybrid reinforced aluminum metal matrix composite for brake disc application: a Taguchi approach. Functional Composites and Structures, 5(1), 015008. https://doi.org/10.1088/2631-6331/acc0d1

[19] Verma, S., Kakkar, V., & Singh, H. (2022). Optimization of Cutting Forces in Dry Turning Process Using Taguchi and Grey Relational Analysis. In Recent Advances in Operations Management Applications: Select Proceedings of CIMS 2020 (pp. 317-334). Singapore: Springer Nature Singapore.

[20] Ochuokpa, E. O., Yawas, D. S., Okorie, P. U., & Sumaila, M. (2021). Evaluation of mechanical and metallurgical properties Al-Si-Mg/mangiferaindica seed shell ash (MSSA) particulate composite for production of motorcycle hub. ATBU Journal of Science, Technology and Education, 9(1), 221-238. https://doi.org/10.13140/RG.2.2.30486.63042

[21] Abifarin, J. K., Olubiyi, D. O., Dauda, E. T., & Oyedeji, E. O. (2021). Taguchi grey relational optimization of the multi-mechanical characteristics of kaolin reinforced hydroxyapatite: effect of fabrication parameters. International Journal of Grey Systems, 1(2), 20-32.
[22] Qi, S., Takagi, Y., Yano, K. I., Kondo, T., Ishikawa, T., & Baba, S. (2024). Derivation of Plunger Injection Input to Prevent Gas Defects by Algebraic Approach for Aluminum Alloy Diecasting. Materials Transactions, 65(6), 657-664. https://doi.org/10.2320/matertrans.f-m2024806
[23] Ibrahim, T. K., Yawas, D. S., Dan-asabe, B., & Adebisi, A. A. (2023). Manufacturing and optimization of the effect of casting process parameters on the compressive strength of aluminum/pumice/carbonated coal hybrid composites: Taguchi and regression analysis approach. The International Journal of Advanced Manufacturing Technology, 125(7), 3401-3414. https://doi.org/10.1007/s00170-023-10923-2
[24] Jayakrishnan, P., & Ramesan, M. T. (2016). Synthesis, characterization and properties of poly (vinyl alcohol)/chemically modified and unmodified pumice composites. Journal of Chemical and Pharmaceutical Sciences ISSN, 974, 2115.
[25] Sharma, A., Sakimoto, N., & Takanohashi, T. (2018). Effect of binder amount on the development of coal-binder interface and its relationship with the strength of the carbonized coal-binder composite. Carbon Resources Conversion, 1(2), 139-146.
[26] Adebisi, A. A., & Ndaliman, M. B. (2015, October). Mathematical modelling of stir casting process parameters for AlSiCp composite using central composite design. In Proceedings of the 28th AGM and International Conference of the Nigerian Institution for Mechanical Engineers organized by The Nigerian Institution for Mechanical Engineers. Nigeria, Abuja City.
[27] Ikubanni, P. P., Oki, M., Adeleke, A. A., & Omoniyi, P. O. (2021). Synthesis, physico-mechanical and microstructural characterization of Al6063/SiC/PKSA hybrid reinforced composites. Scientific Reports, 11(1), 14845. https://doi.org/10.1038/s41598-021-94420-0
[28] Adediran, A. A., Alaneme, K. K., Oladele, I. O., & Akinlabi, E. T. (2020). Wear characteristics of aluminium matrix composites reinforced with Si-based refractory compounds derived from rice husks. Cogent Engineering, 7(1), 1826634.
[29] Sivaiah, P., & Chakradhar, D. (2019). Modeling and optimization of sustainable manufacturing process in machining of 17-4 PH stainless steel. Measurement, 134, 142-152.
[30] Abdulmumin, A. A., Maleque, M. A., & Mohammad, Y. A. (2015). Wear characteristics of multiple particle size silicon carbide reinforced aluminium composite. Advanced Materials Research, 1115, 174-177.
[31] Kok, M. (2005). Production and mechanical properties of Al2O3 particle-reinforced 2024 aluminium alloy composites. Journal of materials processing technology, 161(3), 381-387.
[32] Dagwa, I. M., & Adama, K. K. (2018). Property evaluation of pumice particulate-reinforcement in recycled beverage cans for Al-MMCs manufacture. Journal of King Saud University-Engineering Sciences, 30(1), 61-67.
[33] Ersoy, B., Sariisik, A., Dikmen, S., & Sariisik, G. (2010). Characterization of acidic pumice and determination of its electrokinetic properties in water. Powder Technology, 197(1-2), 129-135. https://doi.org/10.1016/j.powtec.2009.09.005
[34] Pınarcı, İ., & Kocak, Y. (2022). Hydration mechanisms and mechanical properties of pumice substituted cementitious binder. Construction and Building Materials, 335, 127528.
[35] Sahajwalla, V., Zaharia, M., Mansuri, I., Rajarao, R., Dhunna, R., Yunos, F. N., ... & Saha-Chaudhury, N. (2013). The power of steelmaking—harnessing high temperature reactions to transform waste into raw material resources. Iron Steel Technol, 10(8), 68-83.
[36] Gencel, O. (2015). Characteristics of fired clay bricks with pumice additive. Energy and Buildings, 102, 217-224. https://doi.org/10.1016/j.enbuild.2015.05.03
[37] Veeravalli, R. R., Nallu, R., & Mohiuddin, S. M. M. (2016). Mechanical and tribological properties of AA7075–TiC metal matrix composites under heat treated (T6) and cast conditions. Journal of Materials research and Technology, 5(4), 377-383. https://doi.org/10.1016/j.jmrt.2016.03.011
[38] Ujah, C. O., Popoola, P., Popoola, O., Aigbodion, V., & Oladijo, P. (2020). Improving tribological and thermal properties of Al alloy using CNTs and Nb nanopowder via SPS for power transmission conductor. Transactions of Nonferrous Metals Society of China, 30(2), 333-343. https://doi.org/10.1016/s1003-6326(20)65216-5
[39] Baradeswaran, A., & Perumal, A. E. (2014). Study on mechanical and wear properties of Al 7075/Al2O3/graphite hybrid composites. Composites Part B: Engineering, 56, 464-471. https://doi.org/10.1016/j.compositesb.2013.08.013
[40] Baradeswaran, A., Elayaperumal, A., & Issac, R. F. (2013). A statistical analysis of optimization of wear behaviour of Al-Al2O3 composites using Taguchi technique. Procedia Engineering, 64, 973-982. https://doi.org/10.1016/j.proeng.2013.09.174

[41] Prabu, S. B., Karunamoorthy, L., Kathiresan, S., & Mohan, B. (2006). Influence of stirring speed and stirring time on distribution of particles in cast metal matrix composite. Journal of materials processing technology, 171(2), 268-273.
[42] Dan-Asabe, B., Yaro, S. A., Yawas, D. S., & Aku, S. Y. (2019). Statistical modeling and optimization of the flexural strength, water absorption and density of a doum palm-Kankara clay filler hybrid composite. Journal of King Saud University-Engineering Sciences, 31(4), 385-394.
[43] Sivaiah, P., & Chakradhar, D. (2019). Modeling and optimization of sustainable manufacturing process in machining of 17-4 PH stainless steel. Measurement, 134, 142-152.
[44] Rai, A., Mohanty, B., & Bhargava, R. (2016). Supercritical extraction of sunflower oil: A central composite design for extraction variables. Food chemistry, 192, 647-659.